Article

Physical properties of Korean normal aortic valves based on fluid–structure interactions

Jeongrim Choi[1], Jieun Park[2], Junghun Kim[3,*], Jongmin Lee[4,*]

[1] Department of Biomedical Engineering, Kyungpook National University, Daegu 41566, Republic of Korea

[2] Bio-Medical Research Institute, Kyungpook National University and Hospital, Daegu 41940, Republic of Korea

[3] School of Computer Software, Daegu Catholic University, Gyeongsan-si, Gyeongbuk 38430, Republic of Korea

[4] Department of Radiology, School of Medicine, Kyungpook National University & Hospital, Daegu 41944, Republic of Korea

* Corresponding authors: Junghun Kim, fainal2@naver.com; Jongmin Lee, jonglee@knu.ac.kr

Abstract: Recently, numerical methods such as computational fluid dynamics (CFD), have been widely used in heart valve research. The CFD approach has fewer restrictions compared to clinical and experimental methods as it involves interpretations through computer calculations, and it can be used to predict and analyze fluids. For valve numerical analysis using CFD, the mechanical properties of the valve must be defined based on the physical properties. However, most of the existing heart valve numerical analysis studies have been conducted for westerners, and only a few studies on the same topic have focused on Asians. Thus, in this paper, we aim to determine the physical property parameters suitable for defining the mechanical properties of the normal aortic valves of Koreans over time. In this study, we used a fluid−structure interaction technique for the valve simulation and applied three representative valve characteristics presented in previous aortic valve simulation studies. Herein, the valve patency rates in case of simulation and multidetector computed tomography images were compared and analyzed through statistical techniques. Our results revealed that the physical properties, such as density (1050 kg/m^3), Young's modulus (2 MPa), and Poisson's ratio (0.3), are like those of the Korean aortic valve over time. If hemodynamic evaluation of the Korean aortic valve is performed through simulation using these conditions, it can be effective in identifying the factors of heart valve disease.

Keywords: aortic valve; computational fluid dynamics; fluid-structure interaction; valve physical properties

1. Introduction

Cardiovascular disease (CVD) is the leading cause of death worldwide and exhibits a high mortality rate of approximately 32% per year [1]. According to the World Health Organization, the death rate will increase to 22,200 by 2030 [2]. Aortic valve disease is one of the most common CVDs that affect 25% of the population over the age of 65 years [3]. Generally, valve diseases are associated with issues in valve function due to the congenital bicuspid aortic valve or an acquired deformity of the valve structure. Moreover, diseases such as aortic stenosis, calcified aortic valve disease, and valve regurgitation are caused by hemodynamic abnormalities around the valve [4]. Continuous hemodynamic evaluation is necessary for the early diagnosis and prognosis of such aortic valve diseases. In addition, hemodynamic evaluation of functionally defective aortic valves helps us better understand the hemodynamic factors associated with valve disease [5].

In the past few years, several in vivo, in vitro, and in silico studies have been conducted on the hemodynamic evaluation of the aortic valve. In vivo research mainly acquires data from humans or animals and provides only limited data due to high costs and experimental limitations. In vitro research requires the use of expensive and sophisticated equipment to measure data as well as measurements involving limited optical accessibility, especially near valve structures. On the other hand, in silico research is a numerical analysis research method that uses computer simulation such as computational fluid dynamics (CFD). Recently, CFD has gained increasing research interest for understanding the complex physiology of the heart valve [6].

Moreover, in silico research has fewer restrictions compared to in vivo and in vitro research because fluids are analyzed through computer calculations. Additionally, it allows the estimation of hemodynamic and structural details that cannot be measured experimentally, thereby facilitating the evaluation of the impacts of the morphological organization on valve biomechanics [7]. Meanwhile, heart valves have a very complex structure due to changes in hemodynamics according to the shape of the valve, and they move according to the pressure and flow of the heart. Hence, a fluid–structure interaction (FSI) approach that combines CFD and finite element analysis (FEA) can be used for hemodynamic evaluations of the aortic valves [8]. The FSI approach is extensively explored in valve research as it computes and simulates the anatomy related to blood flow and the interaction between the valve [9].

To perform a valve numerical simulation, the mechanical properties of the valve must be defined through physical property parameters such as density, Young's modulus, and Poisson's ratio. The prevalence of valve disease varies by race because Asians and Westerners have differences in physique, thrombotic, and hemorrhagic constitutions, which further generate differences in the mechanical properties of the valves [10,11]. However, most valve numerical simulation studies have defined the physical property parameters for Westerners, and only a few studies on valve physical properties have targeted Asians [12]. Henceforth, the hemodynamics of Asian valves is difficult to evaluate through numerical simulation. However, the Asian valve characteristics need to be defined for the hemodynamic evaluation of Asian valves. In this paper, we have proposed the valve properties targeting Koreans among Asians by comparing various conditions of valve properties, presented in the current valve numerical simulation studies. More particularly, here, we focus on the normal aortic valve physical property conditions that can simulate the mechanical properties of Korean valves over time.

2. Materials and methods

2.1. Aortic valve model

In this study, the shapes of valve movement during heart beats were examined using multidetector computed tomography (MDCT) images of the heart of a healthy male in his 40s. Cardiac MDCT images were acquired using MDCT (SIEMENS, SOMATOM force, Germany) at Kyungpook National University Hospital. A total of 20 different phase images were acquired for the entire cardiac cycle, where a phase image corresponded to the one cycle of contraction, relaxation, and beating of the heart. MDCT images were used in the study with the approval of the Institutional Review

Board (IRB) of the Kyungpook National University Hospital (IRB number: KNUH 2021-01-031).

MDCT images are in Digital Imaging and Communications in Medicine format. Multiplanar reconstruction (MPR) was used to rotate the plane parallel to the valve to obtain short-axis views of the aortic valve [13]. The geometrical parameters of the valve were measured through the short-axis plane of the heart defined by MPR. using the free software MicroDicom (Sofia, Bulgaria). Then, aortic valve models were created by MDCT using the measured geometrical parameters. **Figure 1** shows the reconstructed aortic valve model based on the geometric parameters measured by MDCT. For aortic valve inlet (d_i) and root (d_r), the area was measured and converted to diameter and applied as a two-dimensional model. The area and height of the valve were measured, and the leaflet thickness (h_l) was assumed to be constant at 0.05 cm [14].
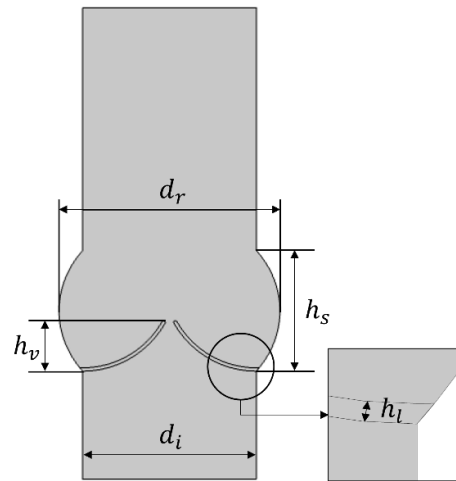

Figure 1. Aortic valve model reconstructed based on geometric parameters.

2.2. Boundary condition

### 2.2.1. Fluid and structure domain

The fluid domain must define boundary conditions and initial conditions for the inlet, outlet, and walls of the blood. For the inlet boundary, the fluid domain was defined as the blood velocity condition at the aortic valve inlet. The ideal aortic valve inlet velocity profile was constructed through MDCT parameters. Velocity time integral (VTI) was derived through stroke volume and left ventricle outflow tract cross-sectional area. The calculated VTI and the time corresponding to the systolic phase were reversely calculated to derive a function as shown in Equation (1). Accordingly, the inlet velocity profile was also constructed. **Figure 2** shows the velocity profile of the aortic valve inlet.

$$f(x) = -5677x^2 + 1703x - 46 \tag{1}$$
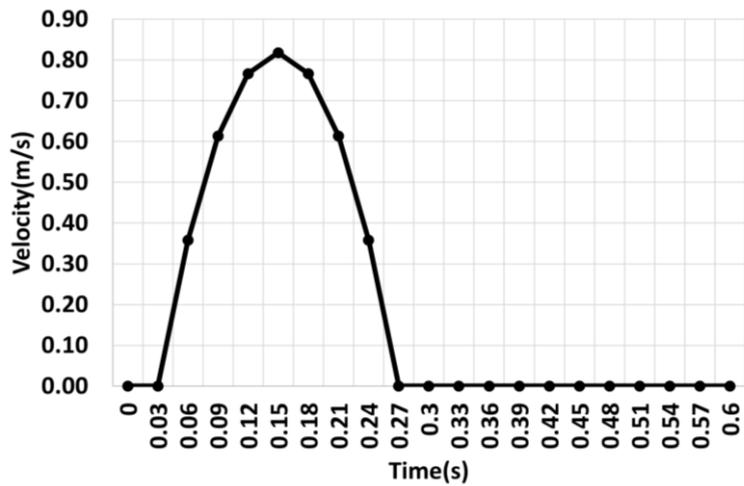
Figure 2. Aortic-valve inlet velocity profile.

The outlet boundary was defined as a pressure condition and assumes a constant pressure of 0 Pa. The wall boundary was set to an anti-skid condition. Moreover, the elasticity of the wall was assumed to be hard and was not considered in this study. The structure domain defined the fixed constraints for the valve and the boundary conditions for the contact. Fixed constraints fixed the contact area between the valve and the wall when the valve was moved by blood. When the valve was actually in contact, it should be fully closed. However, the FSI analysis would result in a heavily distorted mesh, in which the fluid area was separated into structural areas, leading to errors in the simulation run [15]. Hence, the contact condition between the valve leaflet and the symmetric plane was defined to avoid errors, and the offset between the valve leaflets was set at 0.15 cm [16].
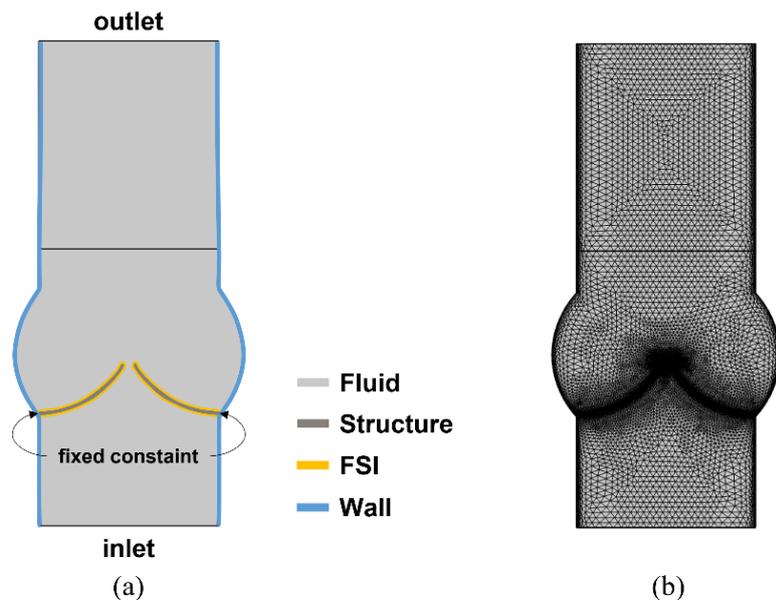

Figure 3. Aortic valve model geometry. **(a)** Boundary condition; **(b)** Domain mesh.

The entire domain was created with a triangular mesh and the valve region was finely meshed using narrow region resolution parameter. The interface between the

wall and the fluid, and between the fluid and solid regions, was created as a boundary layer mesh and fine-tuned using the number of layers and thickness adjustment factor parameters. The mesh applied to the domain was subjected to mesh convergence tests to determine the optimal mesh density. As a result, it consists of 20,220 elements for the fluid and solid domains. **Figure 3** shows the geometry of the aortic valve numerical model, where **Figure 3a** shows the boundary conditions and **Figure 3b** shows the domain mesh.

2.2.2. FSI coupling

The deformed state of the leaflet is changed by the hemodynamic forces of the fluid domain, indicating a strong coupling between the fluid and solid domains. Therefore, fully coupled 2-way FSI coupling approach was adapted to accurately represent the strong interaction between the fluid and solid domains [17]. COMSOL Multiphysics analyzes FSI using the Arbitrary Lagrangian-Eulerian (ALE) method. Generally, flow analysis is performed using Euler's formula, but when the fluid region changes due to structural deformation, the flow grid must be moved, so it is analyzed using the ALE method [18]. **Figure 4** shows the simulation flow chart using FSI analysis. In the simulation, blood flow exerts dynamic forces on the valve, causing deformation of the structure. Valve movements occur within the fluid domain, and these movements degrade the mesh quality of the fluid domain. To improve the mesh quality of the fluid region, a moving mesh was used to smoothen the mesh of the fluid region.
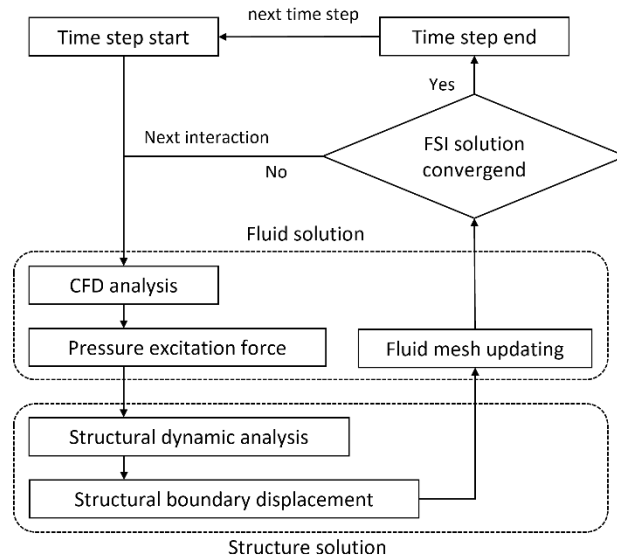
Figure 4. Simulation flow chart of fluid-structure interaction analysis.

2.2.3. Governing equation

The physics interface of COMSOL Multiphysics uses an approach based on the Reynolds Averaged Navier-Stokes (RANS) equations and continuity equations for analyzing incompressible turbulent flow fields and an equation of motion-based approach for analyzing the motion of structures.

$$\rho(\partial u/\partial t) + \rho(u \cdot \nabla)u = \nabla \cdot [-pI + \mu(\nabla u + (\nabla u)^T)] + F \qquad (2)$$

$$\rho \nabla \cdot u = 0 \tag{3}$$

Here, u denotes the velocity of the fluid, ρ denotes the density of the fluid, μ denotes the viscosity of the fluid, I denotes the identity matrix, $(\nabla u)^T$ denotes the turbulent velocity gradient, and F denotes the body force.

$$(4\ \rho(\partial^2 u/\partial t^2) = \nabla \cdot (FS)^T + F_V \tag{4}$$

here u denotes the velocity of the solid and ρ denotes the density of the solid. In addition, $(FS)^T$ denotes the Piola–kirchhoff stress, and F_V denotes the volume force on the undeformed volume. Turbulent flow is expected to appear downstream of the valve at maximal systole when the maximum Reynolds number is approximately 6959 because the pulsatile profile is applied to the aortic valve inlet. Therefore, k–ω based shear stress transfer was used in the turbulent flow model to obtain reliable results, considering flow separation and circulating flow downstream of the valve [19]. The turbulence intensity was set to 1.0% [20], and the turbulence length scale calculated according to Equation (5) was applied.

$$l = 0.07 \times L \tag{5}$$

here l denotes the turbulence length scale and L denotes the inlet diameter. The fluid is defined as blood, which is assumed to be an incompressible Newtonian fluid. The physical properties of blood are defined by density and kinematic viscosity. The density of blood (1060 kg/m^3) was applied, and it is a commonly defined value of blood density. The kinematic viscosity of 0.0032 Pa·s was applied based on the hematocrit of the actual subject and Einstein's formula [21].

2.3. Physical properties of the valve

We entered various combinations of keywords into a search database and utilized a systematic review process used to find articles related to aortic valve numerical simulation [8]. Databases searched included Google Scholar, Web of Science and PubMed. Our search was limited to articles available electronically and published within the last 10 years. Combinations of keywords consisted of FSI, fluid-structure interaction, fluid structure interaction, cardiac, cardiovascular, vascular, aorta, and heart valve. Articles for inclusion met the following criteria: (1) used FSI to investigate a normal cardiac subject, (2) used of a model with linear elastic material properties considering physiological conditions, and (3) was published in English in a peer-reviewed journal. **Figure 5** illustrates the selection process and methodology used in this review. Database search results were initially screened by reviewing titles and abstracts, and the full-text articles were then reviewed for relevance and screened for quality.
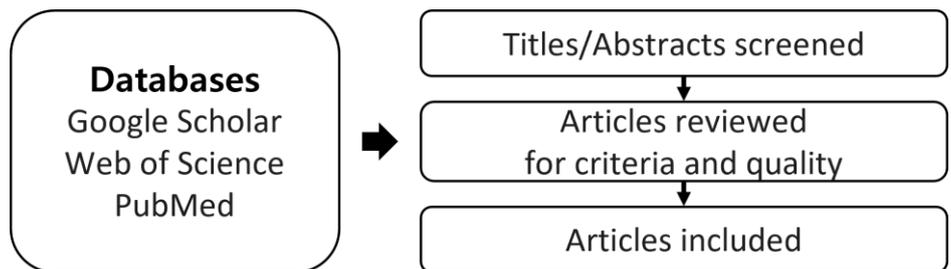
Figure 5. Article review process.

Most articles that met the review criteria were targeted Westerners and used data closest to physiological conditions through experiments and calculations to define physical properties used in the numerical simulation. In this study, representative three valve physical properties conditions presented in the article were applied to this simulation. The conditions for the physical properties of the valve are shown in **Table 1**.

Table 1. Valve material properties.

|	Case 1	Case 2	Case 3
Density	1060 kg/m³	1050 kg/m³	1100 kg/m³
Young's modulus	2 MPa	2 MPa	1 MPa
Poisson's ratio	0.3	0.3	0.45

2.4. Statistics analysis

The degree of agreement in valve opening ratio between the three valve simulations and MDCT was evaluated using the SPSS statistical program, (IBM SPSS Statistics, ver. 26). The error rate was compared with the Kruskal-Wallis test to determine the significance of the valve opening ratio between each simulation and MDCT. The error rate is interpreted as a larger difference between the simulation and the MDCT valve opening ratio with a higher error rate. The Kruskal-Wallis test is interpreted as statistically significant if it is less than the significance level ($p < 0.05$). In addition, Pearson's correlation coefficient and linear regression analysis were performed to determine the effectiveness of the simulation of the mechanical properties of the valve in MDCT. The closer the correlation coefficient to 0, the more is the chances of having no linear relationship. Furthermore, the closer the correlation coefficient to -1, the stronger is the negative relationship, while the closer the correlation coefficient to $+1$, the stronger is the positive relationship. To linear regression analysis, the closer the value of the coefficient of determination (r-square) to 1, the better is the mechanical properties of MDCT expressed in the simulation.

3. Results

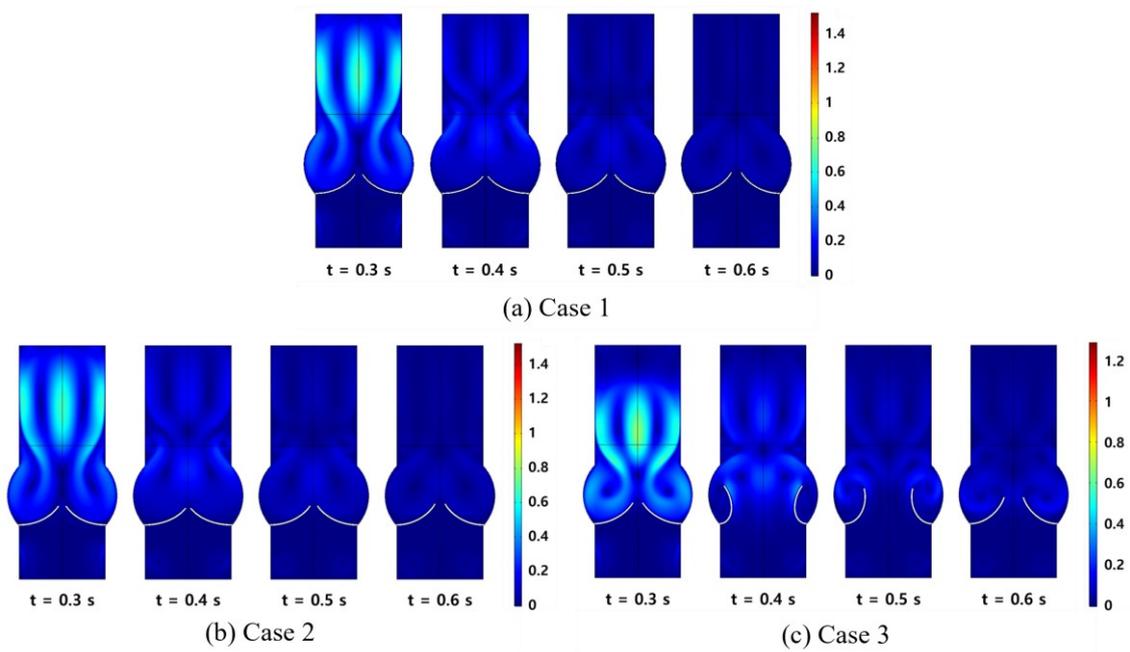### 3.1. Aortic valve simulation qualitative result

Figure 6 shows the velocity contours and streamline results of the simulation for the three physical properties of the systole. During systole, the pressure at the inlet of the flow field increases with the increasing in blood velocity according to the inlet velocity profile, creating a pressure difference between the inlet and outlet, which opens the valve.

Moreover, the laminar flow was observed upstream of the valve, but vortex flow occurred downstream of the aortic sinus after passing the valve leaflet. In addition, the number of vortices, generated in the aortic sinus, increased with the increase in velocity. After $t = 0.15$ s, the blood velocity decreases according to the inlet velocity profile, reducing the pressure difference between the inlet and outlet and closing the valve gradually. The size of the vortex generated during the closing process increases gradually, and the vortex circulates throughout the downstream area.
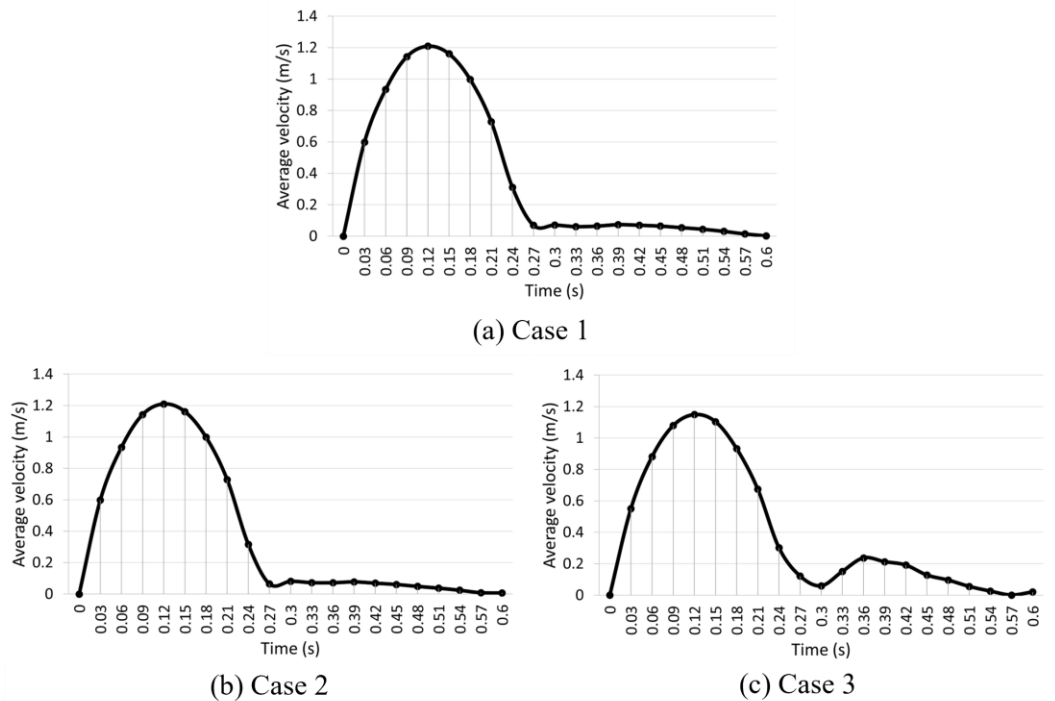
(a) Case 1

(b) Case 2

(c) Case 3
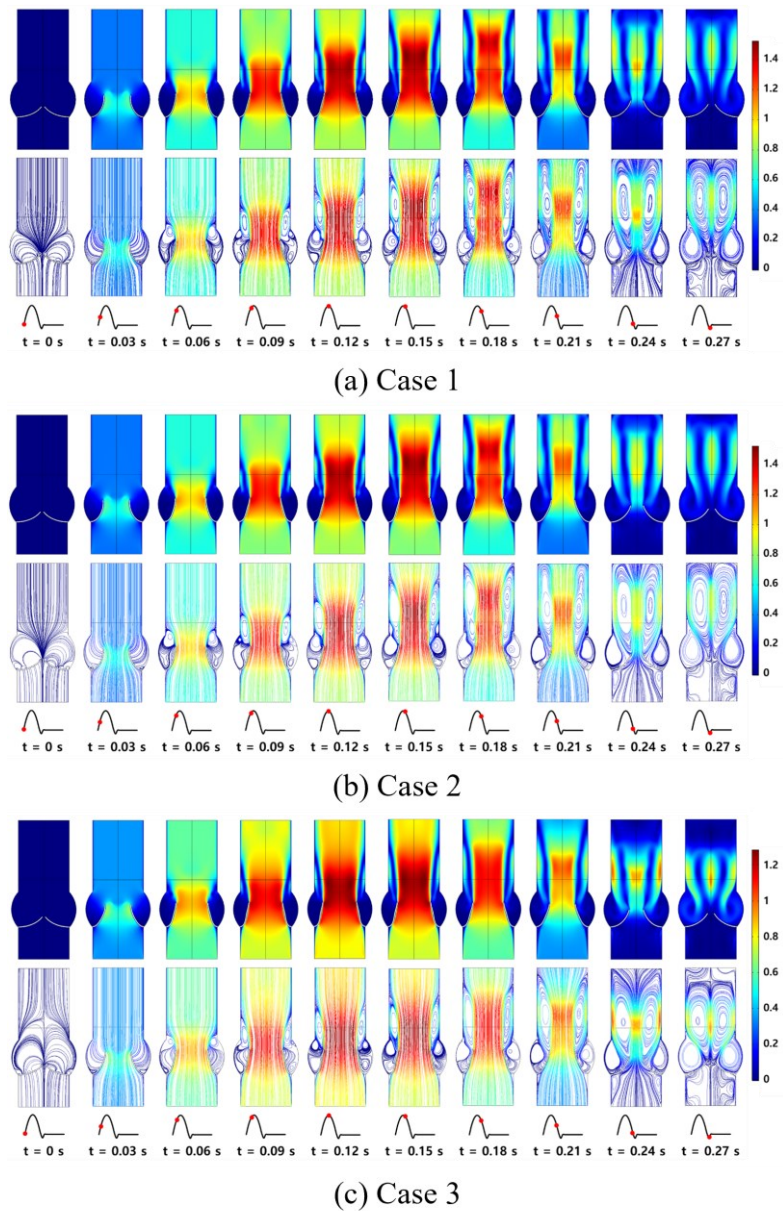
Figure 6. Velocity contour and streamline map of each simulation during systole.

Figure 7 shows the velocity contour results of the simulation for the three physical properties of the diastole. For Case 1 and Case 2, the valve closes as the inlet velocity approaches zero and the pressure difference between the inlet and outlet negatively affects the systole. When the valve is closed, there is no blood flow from the inlet to the aorta, considerably reducing the overall velocity and weakening the vortex generated downstream of the valve over time. For Case 3, the valve reopens after *t* = 0.3 s and does not close resulting in several vortices downstream of the valve. At *t* = 0.6 s, the valve closes again as the vortex moves into the aortic sinus.

Figure 7. Velocity contour map of each simulation during diastole.

3.2. Aortic valve simulation quantitative result

Figure 8. Average velocity graph between valve leaflets.

Figure 8 is a graph of the average velocity measured in the cross-section between the aortic valve lobes. In Case 1, when $t = –0.27$ s, the blood flow velocity changes between 0 m/s and 1.209 m/s. After $t = 0.27$ s, the blood flow velocity tends to decrease at a velocity close to 0. In Case 2, when $t = –0.27$ s, the blood flow velocity changes between 0 m/s and 1.209 m/s. After $t = 0.27$ s, the blood flow velocity tends to decrease

at a velocity close to 0. The above observations indicate that the average velocities of Case 1 and Case 2 showed similar results. However, in Case 3, the blood flow velocity was low, with a maximum of 1.149 m/s. After $t = 0.3$ s, the velocity increases to 0.237 m/s and then decreases again.

3.3. Statistics result

In this study, the valve opening ratios of MDCT and simulations were compared and analyzed using statistical techniques method for three valve physical property conditions. **Table 2** shows the significance level of valve opening rate using the Kruskal-Wallis test. In the Kruskal-Wallis test, the valve opening ratio between the three simulations and MDCT was not significantly above the significance level of the *p*-value.

Table 2. Comparison results of valve opening ratio using the Kruskal-Wallis test.

	p-value
MDCT	
Case 1	
Case 2	>0.05
Case 3	

Table 3 shows the statistical comparison results between MDCT and the three simulations. The error rate was less than 12% in all simulations; Case 3 had the lowest error rate, while Case 2 had the highest error rate. In Pearson's correlation coefficient analysis, all *p*-values showed significant results below the significance level. According to these observations, the three valve characteristics are positively correlated with the valve opening ratio of MDCT and have a high positive correlation value of 0.94 or even higher. In the linear regression analysis, both p-values showed significant results below the significance level. The *r*-square of all three simulations tends to be close to 1. Among them, Case 2 has the highest *r*-square, while Case 3 has the lowest r-square.

Table 3. Comparison and analysis results of valve opening ratio using statistical methods.

		Error ratio	
	Case 1	11.074	
MDCT	Case 2	11.189	
	Case 3	7.057	
			p-value
	Case 1	0.960	
MDCT	Case 2	0.961	<0.05
	Case 3	0.948	
			p-value
	Case 1	0.922	
MDCT	Case 2	0.923	<0.05
	Case 3	0.898	

4. Discussion

In this study, a simulation using FSI analysis was performed to identify normal aortic valve characteristics of Koreans at different times based on the valve characteristics presented in previous aortic valve simulation studies. In addition, statistical techniques were used to compare and analyze the valve patency rates between valve simulated and actual valve images to verify the model.

On the basis of the valve simulation results in systole, all the three simulations exhibit qualitatively similar flow distributions. The comparison of the velocity contour map and the average blood-flow velocity graph shows that Case 1 and Case 2 for the diastole possess physiologically normal mechanical properties with respect to valve. However, Case 3 shows an abnormal pattern, in which the valve reopens in the diastolic period when it should be closed, and the average speed also increases rapidly and then decreases. When compared with Case 1 and Case 2, the physical properties of Case 3 reveal the highest density, lowest Young's modulus, and highest Poisson's ratio. These differences could be because of the differences in physical properties of these three cases. Based on the above results, it is inferred that the physical properties of Case 1 and Case 2 are judged to appropriately simulate the mechanical properties of the actual aortic valve.

Statistical techniques were used to compare valve patency measured by simulation and MDCT. In the Kruskal-Wallis test, the valve opening ratios of simulation and MDCT were not significant, and the three simulations error rates showed a minimum of 7.057% and a maximum of 11.189%. Therefore, not all simulations can be considered to agree with MDCT. Based on Pearson's correlation coefficient analysis, all three simulations described a high positive correlation with MDCT and Case 2, through the highest correlation coefficient. Based on the results of the linear regression analysis, all simulations presented significant results, and Case 2 had the highest r-square value. Case 3 exhibited the lowest error rate and the lowest correlation coefficient, indicating a limited reproduction of the actual mechanical properties. In contrast, Case 2 exhibited a high error rate and the highest correlation coefficient, indicating its ability to reproduce the actual mechanical characteristics. Therefore, since the conditions of Case 2 show the closest shape to the valve opening characteristics of MDCT, the characteristics of the Korean aortic valve opening over time can be best simulated using the physical property conditions of Case 2.

In this study, we tried to present the most similar physical property conditions for Koreans using previously reported valve property conditions. However, the valve characteristics presented in this study cannot be considered to be perfectly suitable for Koreans. Therefore, more research is needed to minimize the difference between simulation and MDCT opening ratio and present new valve property conditions suitable for Koreans by comparing with more cases. In addition, the limitations of the assumptions and methods are described here since the numerical simulation process through FSI is very complex and involves diverse information. First, a two-dimensional aortic valve model was used by measuring parameters based on CT images, rather than a model reconstructed by segmentation from medical images. Numerical simulations using 3D valve models have limited computational time due to computational complexity, and it can be difficult to graphically analyze complex flows

in terms of post-processing and visualization results [22]. Thus, the two-dimensional model was used to reduce the complexity of the numerical simulation and model. Second, the inlet velocity profile of the valve is an idealized aortic valve inlet velocity profile built from CT parameters rather than actual blood flow measurements. Therefore, we believe that the simulation and MDCT can easily be compared.

5. Conclusion

In this study, the mechanical properties of the valve obtained according to the physical properties were compared using the FSI technique to demonstrate the mechanical properties of Korean normal aortic valves over time based on the valve characteristics presented in the valve numerical simulation studies. Our results proved that the mechanical properties most similar to those of the Korean aortic valve of Koreans were characterized by a density of 1050 kg/m^3, Young's modulus of 2 MPa, and Poisson's ratio of 0.3. The hemodynamic evaluation of the aortic valve of Koreans through a numerical simulation using these values are considered to be helpful to identify the factors associated with valve disease.

Author contributions: Conception and design, JC, JP, JK and JL; material preparation, JC; data collection and analysis JC; writing—original draft preparation, JC; writing—review and editing, JC, JP, JK and JL. All authors have read and agreed to the published version of the manuscript.

Ethics approval: The study was conducted in accordance with the Declaration of Helsinki, and approved by the Institutional Review Board (IRB) of Kyungpook National University Hospital (KNUH 2021-01-031). and the IRB exempted consent from the patients, given that it was a retrospective study.

Conflicts of interest: The authors declare no conflict of interest.

References

1. Şahin B, İlgün G. Risk factors of deaths related to cardiovascular diseases in World Health Organization (WHO) member countries. Health & Social Care in the Community. 2020; 30(1): 73-80. doi: 10.1111/hsc.13156
2. Farzadfar F. Cardiovascular disease risk prediction models: challenges and perspectives. The Lancet Global Health. 2019; 7(10): e1288-e1289. doi: 10.1016/S2214-109X(19)30365-1
3. Stewart BF, Siscovick D, Lind BK, et al. Clinical factors associated with calcific aortic valve disease. Journal of the American College of Cardiology. 1997; 29(3): 630-634. doi: 10.1016/S0735-1097(96)00563-3
4. Coffey S, Roberts-Thomson R, Brown A, et al. Global epidemiology of valvular heart disease. Nature Reviews Cardiology. 2021; 18(12): 853-864. doi: 10.1038/s41569-021-00570-z
5. Gould ST, Srigunapalan S, Simmons CA, et al. Hemodynamic and Cellular Response Feedback in Calcific Aortic Valve Disease. Circulation Research. 2013; 113(2): 186-197. doi: 10.1161/circresaha.112.300154
6. Mittal R, Seo JH, Vedula V, et al. Computational modeling of cardiac hemodynamics: Current status and future outlook. Journal of Computational Physics. 2016; 305: 1065-1082. doi: 10.1016/j.jcp.2015.11.022
7. Toma M, Singh-Gryzbon S, Frankini E, et al. Clinical Impact of Computational Heart Valve Models. Materials. 2022; 15(9): 3302. doi: 10.3390/ma15093302
8. Hirschhorn M, Tchantchaleishvili V, Stevens R, et al. Fluid–structure interaction modeling in cardiovascular medicine – A

systematic review 2017–2019. Medical Engineering & Physics. 2020; 78: 1-13. doi: 10.1016/j.medengphy.2020.01.008

9. Abbas SS, Nasif MS, Al-Waked R. State-of-the-art numerical fluid–structure interaction methods for aortic and mitral heart valves simulations: A review. SIMULATION. 2021; 98(1): 3-34. doi: 10.1177/00375497211023573

10. Aluru JS, Barsouk A, Saginala K, et al. Valvular heart disease epidemiology. Medical Sciences. 2022; 10(2): 32. doi: 10.3390/medsci10020032)

11. Kang DY, Ahn JM, Kim JB, et al. Inter-racial differences in patients undergoing transcatheter aortic valve implantation. Heart. 2022; 108(19): 1562-1570. doi: 10.1136/heartjnl-2021-320364

12. Dewi DEO, Hau YW, Khudzari AZM, et al. Cardiovascular Engineering. Springer Singapore; 2020.

13. Kasel AM, Cassese S, Bleiziffer S, et al. Standardized Imaging for Aortic Annular Sizing. JACC: Cardiovascular Imaging. 2013; 6(2): 249-262. doi: 10.1016/j.jcmg.2012.12.005

14. Tango AM, Salmonsmith J, Ducci A, et al. Validation and Extension of a Fluid–Structure Interaction Model of the Healthy Aortic Valve. Cardiovascular Engineering and Technology. 2018; 9(4): 739-751. doi: 10.1007/s13239-018-00391-1

15. Bavo AM, Rocatello G, Iannaccone F, et al. Fluid-Structure Interaction Simulation of Prosthetic Aortic Valves: Comparison between Immersed Boundary and Arbitrary Lagrangian-Eulerian Techniques for the Mesh Representation. Borazjani I, ed. PLOS ONE. 2016; 11(4): e0154517. doi: 10.1371/journal.pone.0154517

16. Hou Q, Liu G, Liu N, et al. Effect of Valve Height on the Opening and Closing Performance of the Aortic Valve Under Aortic Root Dilatation. Frontiers in Physiology. 2021; 12. doi: 10.3389/fphys.2021.697502

17. Benra FK, Dohmen HJ, Pei J, et al. A Comparison of One-Way and Two-Way Coupling Methods for Numerical Analysis of Fluid-Structure Interactions. Swim E, ed. Journal of Applied Mathematics. 2011; 2011(1). doi: 10.1155/2011/853560

18. Abbas SS, Nasif MS, Al-Waked R. State-of-the-art numerical fluid–structure interaction methods for aortic and mitral heart valves simulations: A review. Simulation. 2021; 98(1): 3-34. doi: 10.1177/00375497211023573

19. Stupak E, Kačianauskas R, Kačeniauskas A, et al. The geometric model-based patient-specific simulations of turbulent aortic valve flows. Archives of Mechanics. 2017; 69.

20. Kousera CA, Wood NB, Seed WA, et al. A Numerical Study of Aortic Flow Stability and Comparison With In Vivo Flow Measurements. Journal of Biomechanical Engineering. 2012; 135(1). doi: 10.1115/1.4023132

21. Westerhof N, Stergiopulos N, Noble MIM, et al. Snapshots of Hemodynamics. Springer International Publishing; 2019. doi: 10.1007/978-3-319-91932-4

22. Doost SN, Zhong L, Su B, et al. Two-dimensional intraventricular flow pattern visualization using the image-based computational fluid dynamics. Computer Methods in Biomechanics and Biomedical Engineering. 2016; 20(5): 492-507. doi: 10.1080/10255842.2016.1250891